

Hot carrier cooling in lead halide perovskites probed by two-pulse photovoltage correlation spectroscopy

Yuqing Huang(黄玉清), Chaoyu Guo(郭钞宇), Lei Gao(高蕾), Wenna Du(杜文娜), Haotian Zheng(郑浩天), Da Wu(吴达), Zhengpu Zhao(赵正朴), Chu-Wei Zhang(张楚惟), Qin Wang(王钦), Xin-Feng Liu(刘新风), Qingfeng Yan(严清峰), and Ying Jiang(江颖)

Citation: Chin. Phys. B, 2024, 33 (**10**): 107304. DOI: 10.1088/1674-1056/ad7728
Journal homepage: http://cpb.iphy.ac.cn; http://iopscience.iop.org/cpb

What follows is a list of articles you may be interested in

Improving the electrical performances of InSe transistors by interface engineering

Tianjun Cao(曹天俊), Song Hao(郝松), Chenchen Wu(吴晨晨), Chen Pan(潘晨), Yudi Dai(戴玉頓), Bin Cheng(程斌), Shi-Jun Liang(梁世军), and Feng Miao(缪峰)
Chin. Phys. B, 2024, 33 (**4**): 047302. DOI: 10.1088/1674-1056/ad24d7

Electric modulation of the Fermi arc spin transport via three-terminal configuration in topological semimetal nanowires

Guang-Yu Zhu(祝光宇), Ji-Ai Ning(宁纪爱), Jian-Kun Wang(王建坤), Xin-Jie Liu(刘心洁), Jia-Jie Yang(杨佳洁), Ben-Chuan Lin(林本川), and Shuo Wang(王硕)
Chin. Phys. B, 2024, 33 (**1**): 017305. DOI: 10.1088/1674-1056/ace157

Diamond/c-BN van der Waals heterostructure with modulated electronic structures

Su-Na Jia(贾素娜), Gao-Xian Li(李高贤), Nan Gao(高楠), Shao-Heng Cheng(成绍恒), and Hong-Dong Li(李红东)
Chin. Phys. B, 2023, 32 (**7**): 077301. DOI: 10.1088/1674-1056/acac10

Impact of low-dose radiation on nitrided lateral 4H-SiC MOSFETs and the related mechanisms

Wen-Hao Zhang(张文浩), Ma-Guang Zhu(朱马光), Kang-Hua Yu(余康华), Cheng-Zhan Li(李诚瞻),Jun Wang(王俊), Li Xiang(向立), and Yu-Wei Wang(王雨薇)
Chin. Phys. B, 2023, 32 (**5**): 057305. DOI: 10.1088/1674-1056/acbd2e

Quantum transport signatures of non-trivial topological edge states in a ring-shaped Su-Schrieffer-Heeger double-chain system

Cheng-Zhi Ye(叶成芝), Lan-Yun Zhang(张蓝云), and Hai-Bin Xue(薛海斌)
Chin. Phys. B, 2022, 31 (**2**): 027304. DOI: 10.1088/1674-1056/ac34ff

---

RAPID COMMUNICATION

Hot carrier cooling in lead halide perovskites probed by two-pulse photovoltage correlation spectroscopy

Yuqing Huang(黄玉清)[1], Chaoyu Guo(郭钞宇)[1], Lei Gao(高蕾)[3], Wenna Du(杜文娜)[4], Haotian Zheng(郑浩天)[1], Da Wu(吴达)[1], Zhengpu Zhao(赵正朴)[1], Chu-Wei Zhang(张楚惟)[1], Qin Wang(王钦)[1], Xin-Feng Liu(刘新风)[4,5], Qingfeng Yan(严清峰)[3], and Ying Jiang(江颖)[1,2,6,†]

[1] *International Center for Quantum Materials, School of Physics, Peking University, Beijing* 100871, *China*
[2] *Collaborative Innovation Center of Quantum Matter, Beijing* 100871, *China*
[3] *Department of Chemistry, Tsinghua University, Beijing* 100084, *China*
[4] *CAS Key Laboratory of Standardization and Measurement for Nanotechnology, National Center for Nanoscience and Technology, Beijing* 100190, *China*
[5] *University of Chinese Academy of Sciences, Beijing* 100049, *China*
[6] *Interdisciplinary Institute of Light-Element Quantum Materials and Research Center for Light-Element Advanced Materials, Peking University, Beijing* 100871, *China*

(Received 11 August 2024; revised manuscript received 27 August 2024; accepted manuscript online 4 September 2024)

The next-generation hot-carrier solar cells, which can overcome the Shockley–Queisser limit by harvesting excess energy from hot carriers, are receiving increasing attention. Lead halide perovskite (LHP) materials are considered as promising candidates due to their exceptional photovoltaic properties, good stability and low cost. The cooling rate of hot carriers is a key parameter influencing the performance of hot-carrier solar cells. In this work, we successfully detected hot carrier dynamics in operando LHP devices using the two-pulse photovoltage correlation technique. To enhance the signal-to-noise ratio, we applied the delay-time modulation method instead of the traditional power modulation. This advancement allowed us to detect the intraband hot carrier cooling time for the organic LHP $CH_3NH_3PbBr_3$, which is as short as 0.21 ps. In comparison, the inorganic Cs-based LHP $CsPbBr_3$ exhibited a longer cooling time of around 0.59 ps due to different phonon contributions. These results provide us new insights into the optimal design of hot-carrier solar cells and highlight the potential of LHP materials in advancing solar cell technology.

Keywords: two-pulse correlation spectroscopy, lead halide perovskites, hot carrier cooling, ultrafast dynamics

PACS: 73.20.–r, 73.50.Gr, 78.47.J–, 78.56.–a **DOI:** 10.1088/1674-1056/ad7728

1. Introduction

Hot carriers are the carriers with high energy above the band edges, which are not in thermal equilibrium with the lattice. In solar cells, the hot carriers dissipate their excess energy via carrier–phonon scattering in a sub-picosecond timescale before reaching the band edges for carrier extraction. These thermalization energy losses set a maximum thermodynamic limit, known as the Shockley–Queisser limit, of approximately 34% for a $\sim$ 1.3 eV bandgap at 1 sun AM1.5 for solar to electric power conversion efficiency.[1] To design a new type of solar cell that can overcome the Shockley–Queisser limit, it is crucial to extract hot carriers before they cool to the lattice temperature. Thermodynamic calculations reveal that the conversion efficiencies of these new hot-carrier solar cells in a single junction can reach around 66% under 1 sun illumination.[2] The extraction efficiency of hot-carrier energies depends on the cooling time: the longer cooling time usually leads to the higher efficiency.

Recently, perovskite materials have emerged as promising candidates for hot-carrier solar cells due to their exceptional photovoltaic properties, good stability in air, low cost and ease of production.[3–7] Previous studies on hot carrier cooling in perovskite materials have primarily relied on optical methods, such as time-resolved photoluminescence (TRPL),[8,9] transient absorption (TA),[10,11] pump–push–probe (PPP),[12,13] and so on.[14–16] In this work, we employed the two-pulse photovoltage correlation technique to extract dynamics information in a two-terminal device configuration, which is more relevant to real application. For the first time, we successfully probed the hot carrier cooling process in operando perovskite-based devices.

2. Experimental details

Lead halide perovskite (LHP) materials can provide fundamental insights into the dynamics of photoexcited carriers and their crystals are easy to produce. We grew $CH_3NH_3PbBr_3$ crystals in solution following the procedure described in Ref. [17] and obtained large crystals with sizes up to 5 mm (Fig. 1(a)). To evaluate the quality of the crystal, we used scanning tunneling microscope (STM) to characterize the sample surface at the atomic scale. Imaging organometal halide perovskites using STM has been challenging primarily

†Corresponding author. E-mail: yjiang@pku.edu.cn

© 2024 Chinese Physical Society and IOP Publishing Ltd

due to the difficulty in obtaining a clean, atomically flat surface. The perovskite crystals are typically produced via solution process methods, which are low cost and facilitate large-scale production. However, these processes often result in surface contamination with adsorbates and surface polycrystallinity. We addressed these issues by employing an *in situ* cleaving method under ultrahigh vacuum conditions. This approach allowed us to obtain $CH_3NH_3PbBr_3$ crystals with clean and flat surfaces, which are free of contaminants.

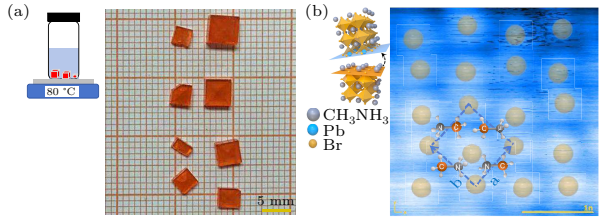


Fig. 1. (a) Optical image of $CH_3NH_3PbBr_3$ crystals with different sizes. Inset: Schematic of the fabrication process of $CH_3NH_3PbBr_3$ crystals. (b) Atomically resolved STM topography image. Image size: 30×30 Å^2, $a = 7.8$ Å, $b = 8.6$ Å. Scan parameters: Bias $= -8$ V and $I = 0.1$ nA. Inset: Schematic of the cleavage process of $CH_3NH_3PbBr_3$ crystals, showing that the CH_3NH_3–Br surface is exposed.

An atomically resolved STM topography image of the $CH_3NH_3PbBr_3$ surface is shown in Fig. 1(b). The large bias (~ -8 V) was used for scanning due to the insulating nature of the sample. The crystallographic plane observed is the (010) surface. The bright protrusions can be assigned to the Br atoms and the intercalated $CH_3NH_3^+$ organic cation is not visible in the STM images according to the previous work.[18,19] These Br atoms are arranged in an alternating fashion, exhibiting short and long interatomic distances, forming a dimer-type structure. This dimer structure arises from the electrostatic interaction between the negatively charged Br^- ions and the dipole of the polarized $CH_3NH_3^+$. The Br^-–Br^- pairs are linked by different sides of the $CH_3NH_3^+$ neighbors. When the positive side of the dipole (the N atom) is nearby, the attractive interaction shortens the Br^-–N distance, driving the pairs of Br ions to get closer. In contrast, the Br ions are repelled by the negative side of the dipole (the C atom). From the STM images, it can be seen that the $CH_3NH_3PbBr_3$ crystal is of very high quality with few defects, making it well-suited for studying the intrinsic optoelectronic properties of the crystal.

3. Results and discussion

In order to extract carrier dynamics information in the true state of operation, we fabricated a simple two-terminal LHP solar cell. This device had a symmetric lateral configuration of Au/LHP/Au, where the Au electrodes with thickness of ~ 50 nm were deposited directly onto the LHP crystals using electron-beam lithography (see the device schematic in Fig. 2(a)).

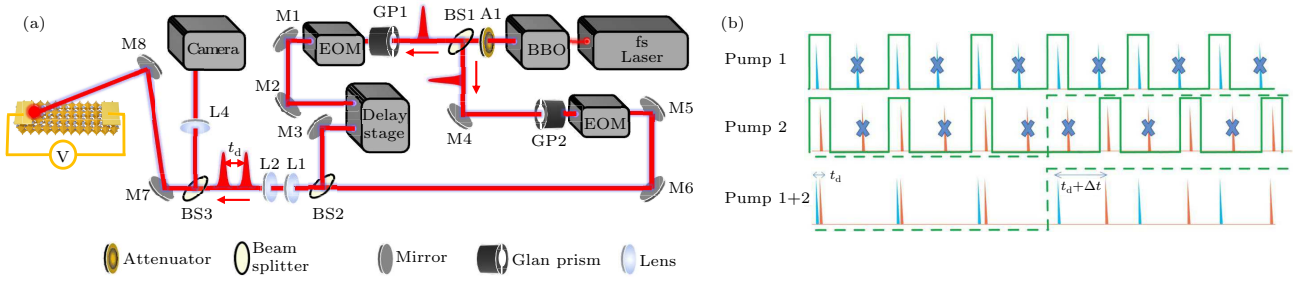


Fig. 2. (a) Illustration of the LHP solar cell device and the laser circuits. (b) Laser pulse manipulation and delay time modulation method, t_d is the time delay and Δt is the delay modulation.

The dynamics measurement system is very similar to an optical pump–probe setup. The system includes two main components: a Ti:sapphire femtosecond laser (MaiTai, pulse width 100 fs, repetition rate 80 MHz) and a CCD camera (see laser circuits in Fig. 2(a)). The femtosecond laser illuminated the electrode–perovskite junction and excited hot carriers. Time-resolved signals were recorded via measuring photovoltages at the electrodes. The CCD camera was used to monitor the focused laser beam through a confocal light path. The time delay between the two laser paths can be adjusted by a high-precision displacement stage (Newport GTS150). The electro optic modulator (EOM) was triggered by a pulse/pattern generator (Agilent 81130A), which was synchronized to the femtosecond laser. The rise time of the EOM was faster than 10 ns. With an edited waveform, individual laser pulses can be selectively passed or blocked (Fig. 2(b)).

Conventional laser power modulation method (such as the one using choppers) can induce inevitable thermal effects, which may obscure weak signals. In order to increase the signal-to-noise ratio, we chose to modulate the delay time. By alternately selecting odd or even numbers of laser pulses (pump 2 in Fig. 2(b)), an AC modulation was added to the delay time (t_d) at a frequency of 300 Hz. As a result, laser pulse pairs with a given delay time (Δt, for example 12.5 ns) at a particular modulation frequency can be obtained. With the help of a lock-in amplifier, the weak photovoltage (V) can be extracted from the background. When T is set to a value much

larger than the relaxation time of the excited state ($t \to \infty$), the lock-in output is simply related to the difference between $V(t)$ and $V(t \to \infty)$.[20] This two-pulse photovoltage correlation measurement is sensitive to the population of the total photoexcited carriers, offering important and unique insights into carrier dynamics.[21]

The band diagram of the Au–$CH_3NH_3PbBr_3$ junction is depicted in Fig. 3(a). Due to the Schottky barrier, there is intrinsic upward band bending near the metal side. Under the laser illumination, electron–hole pairs are photogenerated, quickly relax to the band edges, and then are separated by the built-in electric field, leading to the accumulation of holes on the metal side. These holes decrease the band bending and induce a change in the potential, which is the origin of the photovoltage. The intensity of the photovoltage is related to the population of the photoexcited carriers, allowing us to extract carrier relaxation or recombination dynamics from the photovoltage.[22]

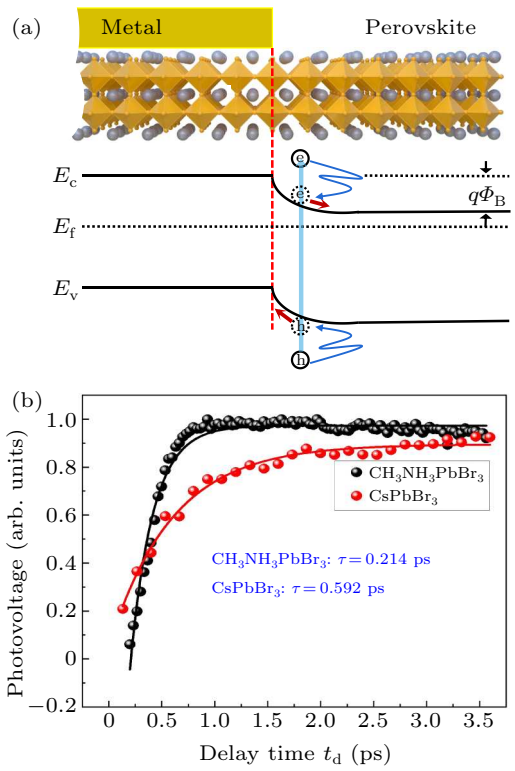


Fig. 3. (a) The energy band diagram (bottom) of the metal–LHP junction (top). The Schottky barrier height is Φ_B (≈ 0.2 eV). The curved arrow means the hot carrier cooling. (b) The measured (symbols) and fitting (solid lines) photovoltage correlation signals $|V(t)|$ are plotted as a function of the time delay t_d. Pump wavelength: 700 nm, fluence: 64 μJ/cm^2. Temperature: 300 K.

Our measurements (Fig. 3(b)) show that the photovoltage is suppressed when the two optical pulses arrive simultaneously due to saturation of the photoresponse. As the time delay between the two pulses increases from zero, the photovoltage starts to recover. The photovoltage recovery, as a function of the time delay, reflects the carrier dynamics of LHP over a wide time scale. Upon the laser illumination, electron–hole pairs are photogenerated within 100 fs. Early-stage processes in the timescale of subpicosecond–picosecond include charge relaxation and interfacial charge transfer, followed by transport and recombination processes occurring in a nanosecond–microsecond timescale.[23] The photovoltage recovery in our measurements exhibits an ultrafast timescale of 0.21 ps, consistent with the intraband cooling time of the hot carriers. The transport and recombination processes are too slow to be detected. This rapid cooling is attributed to the coupling of hot carriers with longitudinal optical (LO) phonons, which establishes thermal equilibrium between the LO-phonon population and the hot carriers.[24,25] This hot carrier cooling time of 0.21 ps is slower than that in most organic semiconductors ($\sim$ 100 fs).[26,27] Potentially, these hot carrier energies could be efficiently extracted before the hot carriers relax to the band edges by optimizing the device configuration.

Additionally, the cation in LHPs plays a critical role in hot carrier cooling. For example, substituting the organic cation with an inorganic counterpart, such as in $CsPbBr_3$ (Fig. 3(b)), increases the hot carrier cooling time to 0.59 ps under the same laser fluence. This trend is congruent with several recent findings in the literatures.[28–30] Along with Thomas' work,[25] we confirm that the phonon scattering is the main channel for hot carrier energy dissipation. Compared to $CsPbBr_3$, $CH_3NH_3PbBr_3$ has more accessible vibrational modes ($< k_BT$) (e.g., 15 in $CH_3NH_3PbBr_3$ versus 9 in $CsPbBr_3$) by breaking the lattice symmetry. These extra coupled cation–lattice modes facilitate faster hot carrier cooling. Considering the diffusion coefficient of 5 cm^2·s^{-1},[31] the estimated diffusion length is around 12 nm in $CH_3NH_3PbBr_3$ and 20 nm in $CsPbBr_3$, making it technically feasible to extract hot carriers.

4. Conclusion and perspectives

By employing the *in situ* cleaving method under ultrahigh vacuum, we characterized the $CH_3NH_3PbBr_3$ crystal surface at the atomic scale using STM. Using an improved delay modulation method, we succeeded in detecting weak signals of hot carrier dynamics in two-terminal LHP devices via the two-pulse photovoltage correlation technique. We found that the intraband cooling time of hot carriers for $CH_3NH_3PbBr_3$ is as short as 0.21 ps. In comparison, the inorganic Cs-based LHPs exhibited a longer cooling time of around 0.59 ps due to the reduced number of phonon modes for carrier–phonon coupling. Our work highlights the critical role of the cation in the hot carrier dynamics of LHPs and underscores the importance of careful materials design for the utilization of hot carriers in prospective photovoltaic applications.

Acknowledgments

Project supported by the National Key R&D Program of China (Grant No. 2021YFA1400500), New Cornerstone Science Foundation through the New Cornerstone Investigator Program, and the XPLORER Prize.

References

[1] Shockley W and Queisser H 2018 *H. Renew. Energy* (Routledge, 2018) pp. Vol2_35–Vol32_54
[2] Ross R T and Nozik A J 1982 *J. Appl. Phys.* **53** 3813
[3] Snaith H J 2013 *J. Phys. Chem. Lett.* **4** 3623
[4] Khatoon S, Yadav S K, Chakravorty V, Singh J, Singh R B, Hasnain M S and Hasnain S M 2023 *Mater. Sci. Energy Technol.* **6** 437
[5] Chowdhury T A, Zafar M A B, Islam M S U, Shahinuzzaman M, Islam M A and Khandaker M U 2023 *RSC Adv.* **13** 1787
[6] Rong Y, Hu Y, Mei A, Tan H, Saidaminov M I, Seok S I and Han H 2018 *Science* **361** eaat8235
[7] Jeong M, Choi I W, Go E M, Cho Y, Kim M, Lee B and Lee J 2020 *Science* **369** 1615
[8] Niesner D, Zhu H, Miyata K, Joshi P P, Evans T J, Kudisch B J and Zhu X Y 2016 *J. Am. Chem. Soc.* **138** 15717
[9] Zhu H, Miyata K, Fu Y, Wang J, Joshi P P, Niesner D and Zhu X Y 2016 *Science* **353** 1409
[10] Yang Y, Ostrowski D P, France R M, Zhu K, Van De Lagemaat J, Luther J M and Beard M C 2016 *Nat. Photonics* **10** 53
[11] Ghosh G, Marjit K, Ghosh S and Patra A 2023 *J. Phys. Chem. C* **127** 8670
[12] Zheng X, Hopper T R, Gorodetsky A, Maimaris M, Xu W, Martin B A and Bakulin A A 2021 *J. Phys. Chem. Lett.* **12** 8732
[13] Feng M, Ye S, Lim J W M, Guo Y, Cai R, Zhang Q and Sum T C 2023 *Small* **19** 2301831
[14] Richter J M, Branchi F, Valduga de Almeida Camargo F, Zhao B, Friend R H, Cerullo G and Deschler F 2017 *Nat. Commun.* **8** 376
[15] Wu X, Tan L Z, Shen X, Hu T, Miyata K, Trinh M T and Egger D A 2017 *Sci. Adv.* **3** e1602388
[16] Nah S, Spokoyny B M, Soe C M, Stoumpos C C, Kanatzidis M G and Harel E 2018 *Nano Lett.* **18** 1044
[17] Tidhar Y, Edri E, Weissman H, Zohar D, Hodes G, Cahen D and Kirmayer S 2014 *J. Am. Chem. Soc.* **136** 13249
[18] Ohmann R, Ono L K, Kim H S, Lin H, Lee M V, Li Y and Qi Y 2015 *J. Am. Chem. Soc.* **137** 16049
[19] Hsu H C, Huang B C, Chin S C, Hsing C R, Nguyen D L, Schnedler M and Chen C W 2019 *ACS Nano* **13** 4402
[20] Terada Y, Yoshida S, Takeuchi O and Shigekawa H 2010 *Nat. Photonics* **4** 869
[21] Sun D, Aivazian G, Jones A M, Ross J S, Yao W, Cobden D and Xu X 2012 *Nat. Nanotechnol.* **7** 114
[22] Wang H, Zhang C, Chan W, Tiwari S and Rana F 2015 *Nat. Commun.* **6** 8831
[23] Shi J, Li Y, Li Y, Li D, Luo Y, Wu H and Meng Q 2018 *Joule* **2** 879
[24] Li M, Bhaumik S, Goh T W, Kumar M S, Yantara N, Grätzel M and Sum T C 2017 *Nat. Commun.* **8** 14350
[25] Hopper T R, Gorodetsky A, Frost J M, Müller C, Lovrincic R and Bakulin A A 2018 *ACS Energy Lett.* **3** 2199
[26] Grancini G, Maiuri M, Fazzi D, Petrozza A, Egelhaaf H J, Brida D and Lanzani G 2013 *Nat. Mater.* **12** 29
[27] Jailaubekov A E, Willard A P, Tritsch J R, Chan W L, Sai N, Gearba R and Rossky P J 2013 *Nat. Mater.* **12** 66
[28] Miyata K, Meggiolaro D, Trinh M T, Joshi P P, Mosconi E, Jones S C and Zhu X Y 2017 *Sci. Adv.* **3** e1701217
[29] Madjet M E, Berdiyorov G R, El-Mellouhi F, Alharbi F H, Akimov A V and Kais S 2017 *J. Phys. Chem. Lett.* **8** 4439
[30] Bretschneider S A, Ivanov I, Wang H I, Miyata K, Zhu X and Bonn M 2018 *Adv. Mater.* **30** 1707312
[31] Wu B, Nguyen H T, Ku Z, Han G, Giovanni D, Mathews N and Sum T C 2016 *Adv. Energy Mater.* **6** 1600551